Global Journal of Science Frontier Research: a Physics and Space Science
Volume 20 Issue 14 Version 1.0 Year 2020
Type : Double Blind Peer Reviewed International Research Journal
Publisher: Global Journals
Online ISSN: 2249-4626 & Print ISSN: 0975-5896

Absorption Properties from Microwire Composite and Films from Microwires and its Application to the Safety Control of Infrastructures

By S. A. Baranov
Shevchenko Pridnestrov'e State University

Abstract- The properties of films made of shielding from a microwire composite and films made of shielding from parallel array of microwires have been studied in the distant diagnostics of dangerous deformations of critical infrastructure objects are investigate. Natural ferromagnetic resonance in glass-coated cast amorphous microwires reveals large residual stresses appearing in the microwire core during castingand external stresses. These stresses, together with magnetostriction, determine the magnetoelastic anisotropy. A correlation between the frequency of natural ferromagnetic resonance (NFMR) (0,1 to 12 GHz), determined from the dispersion of permeability, and alloy composition (or magnetostriction between 1 and 40 ppm) of glass-coated microwires has been systematically confirmed. Absorption of composite (microwire pieces embedded in a polymer matrix) screens has been experimentally investigated. Parallel theoretical studies suggest that a significant fraction of the absorption can be ascribed to a geometrical resonant effect, while a concentration effect is expected for the thinnest microwires. A wide absorption properties profile has been measured from 0.1 to 12 GHz, the form of this profile is ascribed to the presence of natural ferromagnetic resonance (NFMR) in cast glass-coated amorphous magnetic microwires.

Keywords: amorphousmagnetic microwires; ferromagnetic resonance; natural ferromagnetic resonance microwires, radio-absorption shielding; high frequency properties; films from parallel array of microwires.

GJSFR-A Classification: FOR Code: 020399

Strictly as per the compliance and regulations of:

Absorption Properties from Microwire Composite and Films from Microwires and its Application to the Safety Control of Infrastructures

S. A. Baranov

Abstract- The properties of films made of shielding from a microwire composite and films made of shielding from parallel array of microwires have been studied in the distant diagnostics of dangerous deformations of critical infrastructure objects are investigate. Natural ferromagnetic resonance in glass-coated cast amorphous microwires reveals large residual stresses appearing in the microwire core during castingand external stresses. These stresses, together with magnetostriction, determine the magnetoelastic anisotropy. A correlation between the frequency of natural ferromagnetic resonance (NFMR) (0,1 to 12 GHz), determined from the dispersion of permeability, and alloy composition (or magnetostriction between 1 and 40 ppm) of glass-coated microwires has been systematically confirmed. Absorption of composite (microwire pieces embedded in a polymer matrix) screens has been experimentally investigated. Parallel theoretical studies suggest that a significant fraction of the absorption can be ascribed to a geometrical resonant effect, while a concentration effect is expected for the thinnest microwires. A wide absorption properties profile has been measured from 0.1 to 12 GHz, the form of this profile is ascribed to the presence of natural ferromagnetic resonance (NFMR) in cast glass-coated amorphous magnetic microwires.

Keywords: amorphousmagnetic microwires; ferromagnetic resonance; natural ferromagnetic resonance microwires, radio-absorption shielding; high frequency properties; films from parallel array of microwires.

I. Introduction

Interest in magnetic micro and nanowires has greatly increased in the last few years mainly due to their technological applications. Glass-coated amorphous magnetic micro- and nanowires (GCAMNWs) [1-4] are attracting particular attention because of their applicability for multifunctional radioabsorbing shielding (important results published, for example in Refs. [2-20]).

Cast GCAMNWs are produced by the Taylor Ulitovsky method (see in Ref. [1-4]) as depicted in Fig.1. The alloy is heated, in an inductor, up to the melting point. The portion of the glass tube adjacent to melting metal softens, enveloping the metal droplet.

Under suitable conditions, the molten metal fills the glass capillary and a microwire is thus formed, with the metal core completely covered by a glass shell.

The microstructure of GCAMNWs depend mainly upon the cooling rate, which can be controlled when the metal-filled capillary enters a stream of cooling liquid on its way to the receiving coil. Critical quenching rates (10^5-10^7 K/s) for fabrication of amorphous material may be obtained.

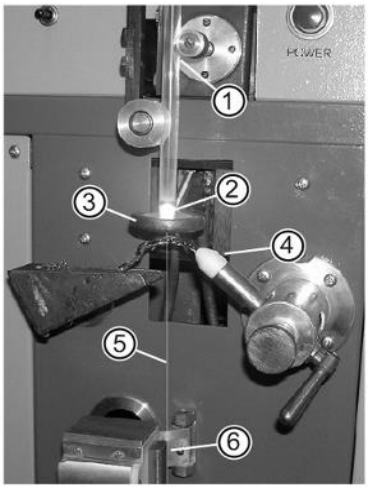

Fig. 1: Process of casting glass-coated amorphous magnetic microwires (see [4] and below).
1. Glass tube. 2. Drop of metal. 3. Inductor. 4. Water. 5. Glass-coated microwire. 6. Rotating support.

The glass coating of the cast GCAMNWs, in addition to protecting the metallic nucleus from corrosion and providing electrical insulation, induces large mechanical stresses in the nucleus. Coupled with its magnetostriction, these determine its magnetoelastic anisotropy, at the origin of a unique magnetic behaviour. The residual stresses are the result of differences in the coefficients of thermal expansion of the metal and of the glass. A simple theory for the distribution of residual stresses was presented in Refs. [2- 8].

Author: Institute of Applied Physics, Academy of Sciences of Moldova, 5 Academia str. MD-2028, Chisinau, Republic of Moldova, Shevchenko Pridnestrov'e State University, str. 25 Oktyabrya 128, Tiraspol, Republic of Moldova. e-mail: sabaranov07@mail.ru

The theory of residual stress is presented in Ref. [4]. We will use results of this theory. Coupled with the magnetostriction of the latter, these factors determine the magnetoelastic anisotropy which is at the origin of a unique magnetic behavior.

In cylindrical coordinates, the residual tension is characterized by the axial, σ_z, radial, σ_r, and tangential, σ_φ, components which are independent of the radial coordinate. The value of these stresses depends on the ratio of the radius, R_m, of the metallic kernel to the total microwire radius, R_c:

$$x = \left(\frac{R_C}{R_m}\right)^2 - 1 \qquad (1)$$

Using the cylinder–shell model, we then obtain a formula for stresses in the metallic kernel of the cast GCAMNWs:

$$\sigma_r = \sigma_\phi \equiv P_\nu , \qquad (2)$$

$$P_\nu = \varepsilon E_1 \frac{kx}{[k(1-2\nu)+1]x + 2(1-\nu)} , \qquad (3)$$

where $P_0 \sim \varepsilon E_1 = \sigma_o \sim 2$ GPa is the maximum stress in the metallic kernel; ε is the difference between the thermal expansion of the metallic core and that of the glass shell with the expansion coefficients α_1 and α_2: ($\varepsilon = (\alpha_1 - \alpha_2)(T^* - T)$); E_1 is the Young modulus of the metal core, T^* is the solidification temperature of the composite in the metal / glass contact region ($T^* \sim$ (800…1000) K), T is the room temperature. The technological parameter k is the ratio of Young's modulus of the glass and the metal:

$k = E_2/E_1 \sim 0.3\ldots0.6$; ν is the Poisson ratio.

Let us consider the case where all the Poisson ratios

$$\nu = 1/3$$

in order to obtain

$$P = \varepsilon E_1 \frac{kx}{(k/3+1)x + 4/3} , \qquad (4)$$

$$\sigma_z = P\frac{(k+1)x+2}{kx+1} . \qquad (5)$$

For materials with positive magnetostriction, the orientation of the microwire magnetization is parallel to the maximal component of the stress tensor, which is directed along the axis of the microwire. Therefore, cast microwires with a positive magnetostriction show a rectangular hysteresis loop with a single large Barkhausen jump between two stable magnetization states and exhibit the phenomenon of NFMR. Equations (1-5) adequately explain the experiments concerning FMR and NFMR (see below).

We suggested a model in which the residual stresses σ_r and σ_z in the GCAMNW monotonically decrease towards the strand axis. This model differs from the models of the standard theory (see Ref. [2-8]).

With additional longitudinal strain, which occurs when the microwire is embedded in a solid matrix that itself deforms under external influence, the following term is added to the expression for the residual axial tension:

$$\sigma_{ez} = \frac{P_o}{S_m(k\ x\ +1)}, \qquad (6)$$

where P_o is the force applied to the composite; S_m is the microwire cross-sectional area; k is the ratio of the Young modulus of the shell to that of the microwire; x is the ratio of the cross-sectional area of the shell to that of the microwire.

For materials with positive magnetostriction, the orientation of the microwire magnetization is parallel to the maximal component of the stress tensor, which is directed along the axis of the wire (see [2-8]). Therefore, cast Fe–based microwires with positive magnetostriction constant show a rectangular hysteresis loop with single large Barkhausen jump between two stable magnetization states and exhibit the phenomenon of natural ferromagnetic resonance (NFMR) (see [2-8]).

The ferromagnetic-resonance (FMR) method is often used for investigation of amorphous magnetic materials (ribbons, wires, thin films). Both macroscopic and microscopic heterogeneity of amorphous materials can be investigated by FMR. Residual stress is an important parameters for amorphous materials which can be studied by FMR (see [1-3]).

FMR is also used for diagnostics of the uniformity of amorphous materials. Extrinsic broadening of FMR lines due to fluctuations of the anisotropy, magnetization, and exchange-interaction constant in amorphous materials has also been investigated. Microwave experiments are very useful for investigation of spin-wave effects. In particular, microwave generation and amplification are of great interest. Investigation of structural relaxation of amorphous materials during heat treatment, using FMR is also important. Differential FMR curves combined with hysteresis curves can give important information in this case.

In the present work, cast glass-coated amorphous microwires with metallic cores and diameters between 0.5 and 25 μm are considered. The amorphous structure of the core was investigated by X-ray methods. The thickness of the glass casing varied between 1 and 20 μm. Using microscopy, we have chosen samples with the most ideal form, and with lengths of about 3-5 mm, for investigation. Microwires

based on iron, cobalt, and nickel (doped with manganese), with additions of boron, silicon, and carbon, were studied. Microwires made from different materials have diverse magnetostriction. We have studied microwire from the same spool, whose glass casing was removed by etching in hydrofluoric acid.

In almost all cases, standard FMR spectrometers from 2 to 32 GHz were used. The magnetic field was measured using a Hall sensor (with accuracy within 0.1 %). In addition, magnetometer measurements determined the magnetization, needed for calculation.

The basic measurements were made in a longitudinal field configuration (external magnetic field was directed along the microwire axis). In this case, a signal of the correct form was obtained from good samples. This gives the possibility of measuring resonant-curve width.

For thick cores, skin effect must be taken into account. In this case the resonant frequency was described by the Kittel formula for a plane (with longitudinal magnetization). The *g* factor was estimated at two resonant frequencies as ~ 2.08 ÷ 2.1 on average. Our results are in good agreement with literature data on the *g* factor for amorphous materials (see Refs. [2-20]). In a transverse field (when the external field is perpendicular to the microwire axis), the signal was weak or not observed in samples with negative magnetostriction. Obviously, the presence of this signal is associated with non-uniformity of the high-frequency demagnetizing factor.

II. Natural Ferromagnetic Resonance

A microwire was considered to be a ferromagnetic cylinder with small radius r. For its characterization we introduce following parameters:

1. The depth of the skin layer is:

$$\delta \sim [\omega(\mu\mu_0)_e\Sigma]^{-1/2} \sim \delta_0(\mu)_e^{-1/2}, \quad (7)$$

$(\mu\mu_0)_e$ is the effective magnetic permeability, and Σ is the microwire electrical conductivity. In the case of our magnetic microwires, with the relative permeability $|\mu|$ near resonance of the order 10^2, ($\omega \sim$ (8 ÷ 10) GHz) δ changes from1 to 3 μm.

2. The size of the domain wall (according to Landau-Lifshits theory) is:

$$\Delta \sim (A/K)^{1/2} \sim (10 \div 0{,}1)\ \mu m, \quad (8)$$

where *A* is the exchange constant and *K* is the anisotropy energy of the microwire ($K \sim \lambda\sigma$, where λ is the magnetostriction constant and σ is the effective residual stress from the fabrication procedure (see Refs. [2, 4] and Eqs. (1-6))). The full theory gives $\Delta_f \sim 0{,}1\mu m$ for the size of the domain wall of glass-coated microwires (see Ref. [4]).

3. The radius of a single domain (according to Brown theory) is

$$a \sim A^{1/2}/M_S \sim (0{,}1 \div 0{,}01)\ \mu m, \quad (9)$$

where M_s is the saturation magnetization of microwire.

According to Refs. [2-8] the frequency of the *NFMR*is:

$$\left(\frac{\omega}{\gamma}\right)^2 = \left(H_e + 2\pi M_S\right)^2 - \left(2\pi M_S\right)^2 \exp\{-2\delta/r\}, \quad (10)$$

where γ is the gyromagnetic ratio ($\gamma \sim 3$ MHz/Oe). The anisotropy field is $H_e \sim 3\lambda\sigma/M_s$(for exact calculations of anisotropy field, see below).

If $r < \delta$, we have:

$$\frac{\omega}{\gamma} = H_e + 2\pi M_S \quad (11)$$

If $r > \delta$, the *NFMR* frequency is given by (see Refs. [2 - 8]):

$$\left(\frac{\omega}{\gamma}\right)^2 = H_e\left(H_e + 4\pi M_S\right). \quad (12)$$

The discovery of natural ferromagnetic resonance (*NFMR*) in amorphous microwires [2] was preceded by their study using standard *FMR* methods [4-7]. Then, the shift in the resonant field, due to core deformation of the microwire associated with fusing the glass and core at the temperature of microwire formation, was observed. The *FMR* line width is also of interest because it characterizes, in particular, the structural parameters [2-18].

Since the skin penetration depth of a microwave field in a metallic wire is relatively small in comparison with its diameter the resonant frequency of *FMR* can be determined by means of Kittel formula (Eq. (12)). Taking into account the magnetoelastic stress field [2, 3], for a thin film magnetized parallel to the surface, we can obtain:

$$\left(\frac{\omega}{\gamma}\right)^2 = \left[H + (N_Z' - N_X')M_S + 4\pi M_S)\right]$$

$$\times (H + (N_Z' - N_Y')M_S), \quad (13)$$

where *H* is the FMR field; N_X', N_Y', N_Z' are components of tensor of effective demagnetizing factors in case of magnetoelastic stress:

$$N_i' = \frac{3|\lambda|\sigma i}{2M_S^2}\left(\cos^2\theta i - \frac{1}{3}\right); \quad (14)$$

where:

$$\theta_1 = \theta_2 = 90^\circ, \theta_3 = 0.$$

Components σ_i (see Eqs. (1-6)) are residual stresses (see in Ref. [2, 3]). Then,

$$N'_X = N'_Y = -\frac{|\lambda| P}{2M_S^2};$$

$$N'_Z = \frac{|\lambda| P}{2M_S^2}\frac{(k+1)x+2}{kx+1}; \quad (15)$$

Substituting the σ_i values obtained in our previous works [3-8] (see Eqs. (1-6)), and taking into account Eqs. (13), (14), we can calculate conditions for *FMR*:

$$\left(\frac{\omega}{\gamma}\right)^2 = \left[H + \frac{(3|\lambda|P)}{2M_S}\frac{x\left(k+\frac{2}{3}\right)+\frac{5}{3}}{kx+1} + 4\pi M_S\right]$$

$$\times\left[H + \frac{(3|\lambda|P)}{2M_S}\frac{x\left(k+\frac{2}{3}\right)+\frac{5}{3}}{kx+1}\right]. \quad (16)$$

If the glass is removed, the stress is completely removed. Then the *FMR* resonant field of wire without glass casing, H_0, is determined from:

$$\left(\frac{\omega}{\gamma}\right)^2 = H_0\left(H_0 + 4\pi M_S\right). \quad (17)$$

We have shown (see Ref. [1-4, 6-8]) that these relations quantitatively explain all of the basic features of *NFMR* and *FMR*. Note that the value of M_S required for the calculations was determined both by standard methods on a vibration magnetometer and with the use of interpolation formulas given here. The error relative to tabular values for the given alloys is not greater than 5%.

For the frequency of *NFMR* under the simple approximation taking $\varepsilon E_1 \sim 2$GPaand $k \sim 0.4$ this formula can be written as:

$$\omega(GHz) \approx \omega o\left(\frac{0.4x}{0.4x+1}\right)^{1/2},$$

$$\omega o(GHz) \approx 1{,}5\left(10^6\lambda\right)^{1/2}. \quad (18)$$

As you can see, dependence for the frequency of NFMR (Eqs. (18), and Figs 2, 3, 4) is determined from two typical values, x, λ.

The basic contribution to the NFMR frequency and NFMR line width is due to the effective magnetostriction and parameter x (Eqs. (18), and Figs. 2-4).The residual stress in the microwire plays the dominant role in the formation of the absorption line width, as it will be shown below(Figs 5, 6).

The NFMR frequency in the distant diagnostics of dangerous deformations of critical infrastructure objects can be written as

$$\omega(GHz) \approx \omega o\left(\frac{0.4x}{0.4x+1} + \frac{\sigma_{ez}}{\sigma_o}\right)^{1/2}, \quad (18a)$$

where

$$\omega_o(GHz) \approx 1{,}5(10^6\lambda)^{1/2}$$

These formulas allow you to determine stress in the distant diagnostics of dangerous deformations of critical infrastructure objects such as bridges, dams, wind turbine towers, skyscrapers, stack-furnaces, embankments, etc. To this end, fragments of magnetic microwires will be embedded in the bulk of concrete structures or on their surface during construction or after it by means of coating with a special concrete-adhesive plaster.

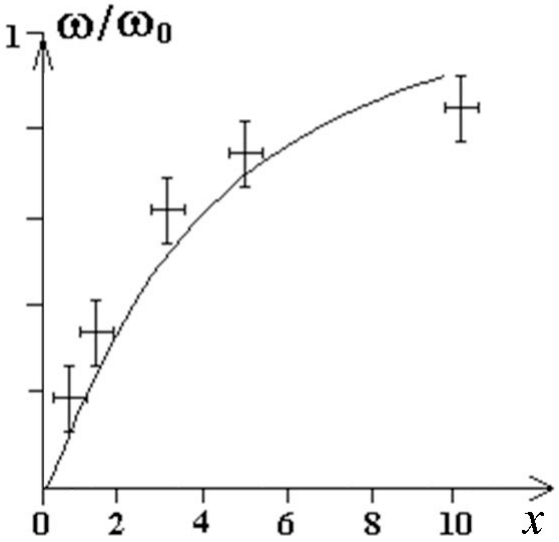

Fig. 2: Theoretical curve of *NFMR* frequency as a function of x (according to Egs. (16) – (18)) and experimental data (see [2])

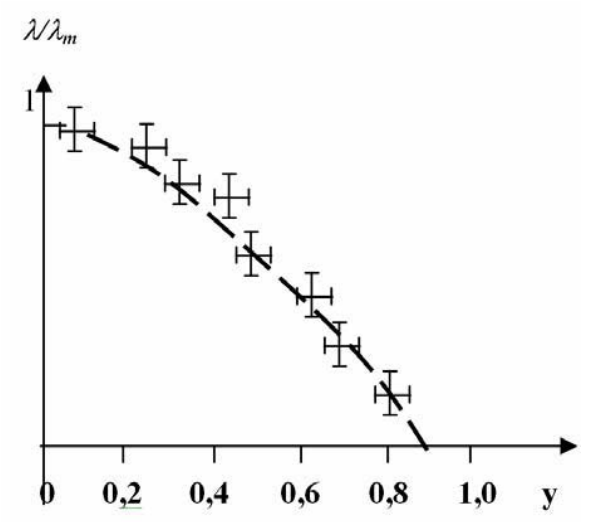

Fig. 3a: Dependence of relative magnetostriction λ/λ_m for alloy composition $(Co_y\ Fe_{1-y})_{75}(BSiC)_{25}$ series cast glass-coated amorphous magnetic microwires according to Eqs. (16) – (18), where y = Co/(Co+Fe) (see [2])

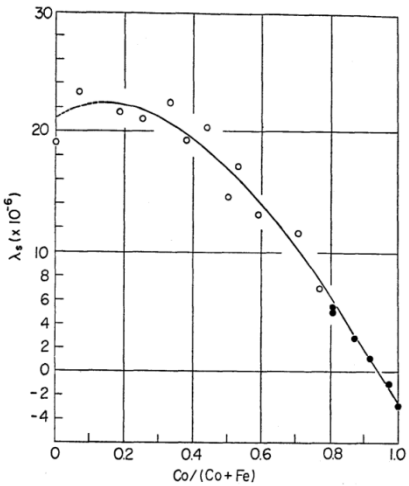

Fig. 3b: Typical saturation magnetostriction λ_s in the amorphous Co –Fe alloys: ○$(Fe_{1-y}Co_y)_{80}(PC)_{20}$;

●$(Fe_{1-y}Co_y)_{75}(SiB)_{25}$(according to Ref. [2]).

When the penetration depth of the microwave field in the metallic wire is small relative to the wire diameter (on account of the skin effect), the resonant frequency in *FMR* and *NFMR* may be determined by means of Eqs. (1-6).(The general theory of residual tension is presented in Refs. [2, 4], but here it is enough to use the simple theory from [3])

Substituting typical values of λand *x*in Eq. (18) we reach numerical values of *NFMR* in a range from 1 to 12 GHz. A systematic study on the *NFMR* frequency for the alloy series $(Co_yFe_{100-y})_{75}(BSiC)_{25}$ has been performed as a function of the Co content (Fig.3). The magnetostriction has then been evaluated using Eq. (18). The result is plotted in Fig. 3a which shows good agreement with the magnetostriction values as determined through conventional techniques (Fig3b.). Thus, the final theory quantitatively explains all the basic features of *NFMR* and *FMR*. However the area of experimental research in the case of small radius of a metallic nucleus radius of a microwire remains vacant.

III. Radio-Absorption Shielding

The designs of composites from GCAMNWs have following configurations.

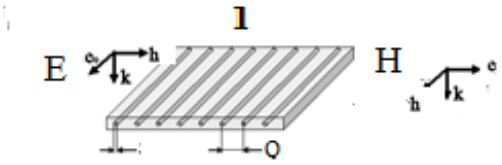

Fig. 4a: Composite shielding for radio absorption protection with GCAMNWs where were maked in grating form. We can consider two types of orientation of a magnetic field: E and H

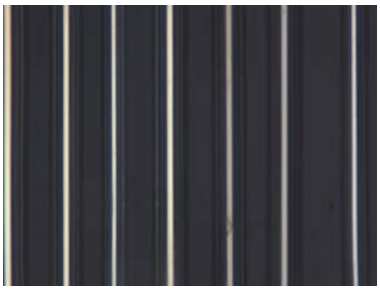

Fig. 4b: Diffraction grating with GCAMNWs

Fig. 4b: Composite shielding for radio absorption protection with GCAMNWs where were made ina stochastic mixture of microwires in the polymeric matrix

Natural ferromagnetic resonance (*NFMR*)occurs when the sample is submitted to a microwave field without application of any biasing field other than the intrinsic anisotropy field of the microwire.

Near the natural ferromagnetic resonance frequency, Ω, the dispersion of permeability μ. given by

$$\mu(\omega) = \mu'(\omega) + i\mu''(\omega), \qquad (19)$$

exhibits a peak in μ" and a zero crossing of μ' .

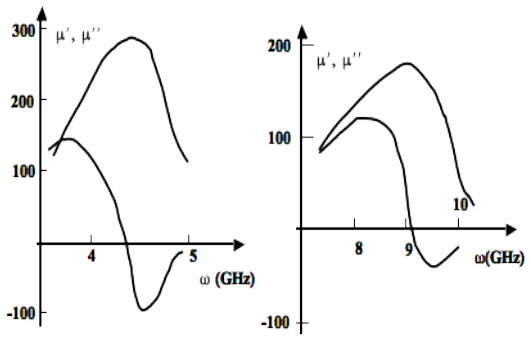

a b

Fig. 5: Real and imaginary relative permeability components around NFMR for $Co_{59}Fe_{15}B_{16}Si_{10}$ (a) and $Fe_{69}C_5B_{16}Si_{10}$ (b) microwires ($r \sim 5\mu m$, $x > 8$ (see [2, 5])

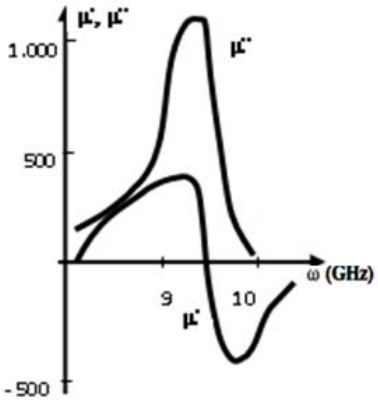

Fig. 5c: Frequency dispersion of the real and imaginary parts of the relative permeability around the NFMR frequency for the $Fe_{68}C_4B_{16}Si_{10}Mn_2$ microwire ($R_m \sim 5\ \mu m$, $x \sim 5$)(see [19]).

Figures 5a, 5b and 5c show resonance frequencies of 4.4; 9.0 and 9.5 GHz, and resonance widths of 1,5; 1 and 0.5 GHz. Near resonance, μ'' is expected to be described by

$$\mu''/\mu_{dc} \sim \Gamma\Omega / [(\Omega - \omega)^2 + \Gamma^2], \qquad (20)$$

where μ_{dc} is static magnetic permeability and Γ is the width of the resonant curve. Very near resonance,, when $\Gamma > (\Omega - \omega)$, Eq. (20) reduces to

$$\mu''/\mu_{dc} \sim \Omega / \Gamma \sim (10 \div 10^2).$$

Note that in Fig. 5a the imaginary component is rather symmetrically distributed around the resonance frequency. This is due to the symmetric distribution of the circular permeability in the near surface layer, within the penetration depth. In contrast, in Figs. 5b, 5c the imaginary component shows a non-symmetric feature around the resonance frequency. This can be attributed to the inhomogeneous character of the permeability in the region close to the surface of the microwire where metastable phases form, as demonstrated by X-ray studies.

Monitoring the geometry of the microwire (i.e., its diameter) and the magnetostriction through its composition enables one the fabrication of microwires with tailor able permeability dispersion and for creating Radioabsorption materials:

1. Determining the resonant frequency in a range from 1 up to 12 GHz;
2. Controlling the maximum of the imaginary part of magnetic permeability.

High-frequency properties, pieces of microwires have been embedded in planar polymeric matrices to form composite shielding for radio absorption protection. Experiments have been performed employing commercial polymeric rubber around (2 ÷ 3) mm thick. Microwires are spatially randomly distributed within the matrix before its solidification. Concentration is kept below (8 ÷ 10) g of microwire dipoles (1 ÷ 3)mm long) per 100g rubber [2, 6, 7]. A typical result obtained in an anechoic chamber is shown in Fig. 6a for a screen with embedded $Fe_{69}C_5B_{16}Si_{10}$microwires.

As observed, an absorption level of at least 10 dB is obtained in the frequency range from 8 to 12 GHz with a maximum attenuation pick of 30 dB at around 10 GHz. In general, optimal absorption is obtained with microwires with metallic nuclei of diameter $2r = (1 \div 3)$ μm ($2R \sim 20\mu m$ ($x > 10$)) and length $L = (1 \div 3)$ mm. Such pieces of microwires can be treated as dipoles whose length, L, is comparable to the half value of the effective wavelengths, $\Lambda_{eff}/2$, of the absorbed field in the composite material (i.e., in connection to a geometric resonance).

Fig. 6a also shows how the frequency absorption spectrum of shielding with $Fe_{69}C_5B_{16}Si_{10}$ microwires changes when it is rotated (90° each spectrum). We attribute the changing attenuation to the lack of perfect angular distribution of microwires which length not always fit within the shielding thickness.

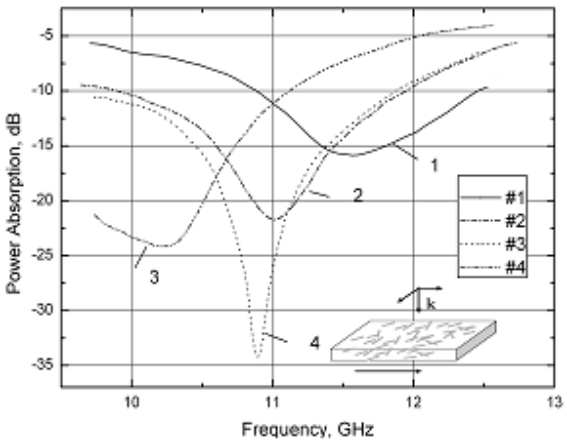

Fig. 6a: Absorption characteristics of shielding by a microwire composite with *NFMR* in the *HF* - field in the range of frequencies 10-12 GHz. Curve 1 represents an initial situation of the screen; then 2, 3, 4: the screen is turned by 90° about a perpendicular axis each time

The effect doesn't even have mirror symmetry.

(The measurement error was less than 10% for the frequency, and while the spread of the attenuation factor was 5 dB).

Small fluctuations in concentration of dipoles at a concentration of dipoles near the percolation threshold can lead to fluctuation of the absorption curve. Similar results were presented in [2].

As observed, both frequency dependences (Fig. 5b and 6) are similar except for the half-width value of the permeability.

Although the design of absorption shielding can be based on disposing the dipolar pieces in a stochastic way, we consider, for simplicity, a theoretical analysis for a diffraction grating (see Fig 6b) with spacing between wires Q $<\Lambda$ (Λ is wavelength of absorbed field).(Another simple example is in Appendix A).

The propagation of an electromagnetic wave through absorption shielding with microwire-based elements is characterized by transmittance, $|T|$, and reflectance, $|R_r|$, coefficients given by:

$$|T| = (\alpha^2 + \beta^2)/[(1+\alpha)^2+\beta^2];$$

$$|R_r| = 1/[(1+\alpha)^2+\beta^2], \qquad (21)$$

where $\alpha=2X_r/Z_0$, and $\beta=2\,Y/Z_0$, with $Z_0=120\pi/Q$, and the complex impedance $Z= X_r + iY$.

The absorption function, G, is correlated with the generalized high-frequency complex conductivity Σ (or high-frequency impedance Z).

Here, we use the analogy between the case of a conductor in a waveguide and that of a diffraction grating. The absorption function, given by:

$$|G| = 1 - |T|^2 - |R_r|^2 = 2\alpha / [(1+\alpha)^2+\beta^2], \qquad (22)$$

Has a maximum,

$$|G_m| = 0{,}5 \geq |G|,$$

for simultaneous $\alpha=1$, and $\beta=0$, for which

$$|T|^2 = |R_r|^2 = 0{,}25.$$

The minimum, $|G|=0$, occurs at $\alpha=0$, β any positive number).

Theoretical estimations taking into account only the active résistance of microwires result in attenuation within the range (5 ÷ 15) dB being much lower than experimental results, which for spacing of microwires Q $=10^{-2}$ m ranges between 18 and 15 dB, while for a spacing Q = 10^{-3} m it increases up to 20 to 40 dB. Thus, it becomes clear that shielding exhibit anomalously high absorption factors, which cannot be explained solely by the resistive properties of microwires.

The high-frequency conductivity, Σ_m, of a stochastic mixture of microwires in the polymeric matrix can be expressed as a function of the conductivities, Σ_i, of non-conducting (polymeric matrix) and conducting (microwire) elements, denoted by sub-indices 1 and 2, respectively, as [2]:

$$\Sigma_m = B + (B^2 + A\Sigma_1\Sigma_2)^{1/2}, \qquad (23)$$

where

$$B=1/2\{[\Sigma_1(X_1-AX_2)+\Sigma_2(X_2-AX_1)];$$

X_i is fractional volume:

$$(X_1+X_2)=1;$$

$$A=1/(J_1-1), \text{ with } \quad J_1 \sim (J+Y/X_r)$$

being the fractal dimension of the system (J is the geometrical dimension of the system) and

$$Y/X_r \sim (r/\delta)^2.$$

Fig. 7 shows that in case of a thick microwire ($r > \delta \approx 1\mu$m), the conductivity of the system becomes very large, even in case of small microwire concentration, indicating the case of an antenna resonance as reported in [2].

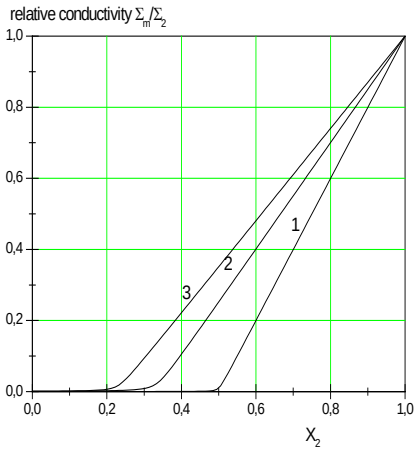

Fig. 7: Generalized conductivity calculated using formula (23) for $\Sigma_2 / \Sigma_1 \sim 10^4$

1 thin microwire ($r<\delta\sim1$ μm) J =2, Y =0
2 thin microwire ($r<\delta\sim$ 1 μm) J =3, Y =0
3 thick microwire ($r>\delta\sim1$ μm) J_1 =4, Y/X_r = 1

Let us consider the effective absorption function, (as in Eq. (22)):

$$|G_{eff}| \sim \Gamma_{eff}\Omega_{eff}/ [(\Omega_{eff}- \Omega)^2 + \Gamma_{eff}^2], \qquad (24)$$

where $\Gamma_{eff} \geq \Gamma$ (see Eq. (12)) and $\Omega \sim \Omega_{eff} = 2\pi c/\Lambda$.

A microwave antenna will resonate when its length, L, satisfies

$$L \sim \Lambda/ 2(\mu_{eff})^{1/2}. \qquad (25)$$

The maximum absorption (see Fig 6) occurs for $\Omega_{eff} \sim 10$ GHz ($\Lambda \sim 3$ cm) and $\mu_{eff} \sim 10^2$, (according to Fig. 5). This corresponds to:

$$L \sim (1{,}5 \div 2) \text{ mm}, \qquad (26)$$

when the microwire concentration((see Fig.7) X_2<0,2) is much less than the percolation threshold.. A greater concentration of dipoles increases absorption, $|G_{eff}|$, but also increases reflectance, $|R_{r1}|$, which can be simply evaluated to be [2]:

$$|R_{r1}| \sim 1 - 2\sqrt{(\Omega/2\pi\Sigma_m)}, \quad (27)$$

where $\Omega/2\pi \sim 10^{10}$ Hz.

The formula is applicable, and calculation of small reflectance, $|R_{r1}|$ is possible, only if

$$\Sigma_m \sim 10^{11} Hz,$$

for concentration below the percolation threshold (as $\Sigma_2 \sim 10^{15}$Hz).

Thus, for very thin microwires (i.e., thinner than 1 μm diameters) embedded in a composite matrix with concentration larger than the percolation level $X_2 \sim 0,2$ a noticeable absorption effect should be expected.

Atypical result obtained in an anechoic chamber is shown in Fig. 8 for radio-absorbing shielding with embedded $Fe_{68}C_4B_{16}Si_{10}Mn_2$ microwires. As observed, an absorption level of at least 10 dB is obtained in a frequency range of (8…12) GHz with a maximum attenuation peak of 30 dB at about 10 GHz. In general, optimal absorption is obtained for microwires with metallic kernels of diameter $2R_m \sim 10$ μm ($x \sim 5$) and length L = (1…2) mm. These micro wire pieces can be treated as dipoles whose length L is comparable to the half value of the effective wave lengths $\Lambda_{eff}/2$ of the absorbed field in the composite material (i.e., in connection to a geometric resonance). A similar result has been received for radio-absorbing shielding with a different GCAMNW (see Refs. [2-8]).

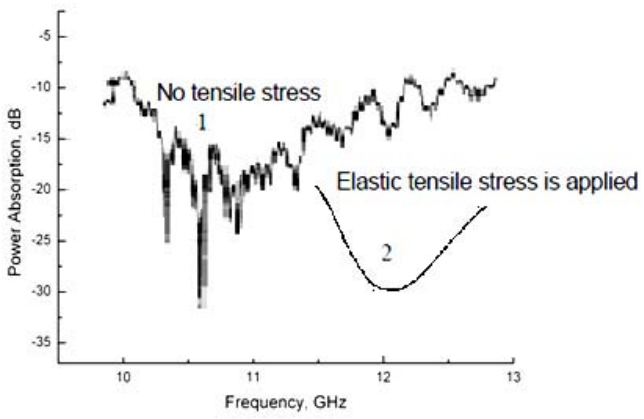

Fig. 8a: 1–Average absorption characteristics of a shielding containing a microwire composite exhibiting NFMR at microwave frequencies ranging from (10…12) GHz for $Fe_{68}C_4B_{16}Si_{10}$ Mn_2 microwires ($R_m \sim$ 5 μm, $x \sim 5$).
2 – Absorption curve in case of anexternal pressure.
(see Ref. [19])

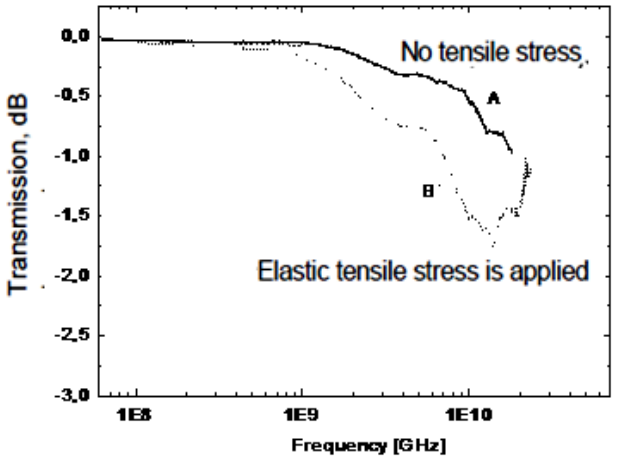

Fig. 8b: A – Average absorption characteristics of diffraction grating with GCAMNWs exhibiting NFMR at microwave frequencies ranging from (1…10) GHz for $Co_{65}Fe_{10}B_{15}Si_{10}$ microwires ($R_m \sim$ 5 μm, $x \sim 5$)

B – Absorption curve in case of anexternal pressure.

IV. Final Remarks

One of the important technological features of the GCAMNWsis the high rate of cooling and solidification of the composite fibers drawn from the molten alloy and consisting of a ferromagnetic metal core and a glass coating. Significant differences between the thermal expansion coefficients of the glass and metal alloy lead to the appearance of large residual stresses.

Particular attention has been paid to the parameters determining the anisotropy of cast GCAMNWs. The continuous casting of GCAMNWs (Taylor-Ulitovsky method) has some limitations, determined by the physical properties of metal and glass (see Ref. [2]).

We have presented simple analytical expressions for the residual stresses in the metallic kernel of the microwire, which clearly show their dependence on the ratio of the external radius of the microwire to the radius of the metal kernel and on the ratio of Young's modules of glass and metal. Our modeling based on the theory of thermoelastic relaxation, shows that the residual stresses increase from the axis of the microwire to the surface of its metallic kernel, which is in accordance with the previously obtained experimental data (see Ref. [2]). Thus, in the manufacture of cast microwires with a glass coating by the Taylor-Ulitovsky method, the residual stresses reach maximum values on the surface of the metal core (see Refs. [2-8]).

The cast GCAMNWs exhibit natural ferromagnetic resonance (NFMR), whose frequency depends on the composition, geometrical parametersand deformationof the microwire. The NFMR

phenomenon observed in glass-coated magnetic microwires opens up the possibility of developing new radio-absorbing materials with a wide range of properties. An important feature of cast microwires with an amorphous magnetic core is the dependence of the NFMR frequency on the deformation (stress effect). In this regard, the microwave response of a composite consisting of segments of amorphous magnetic microwires with a glass coating in a flat dielectric plate is investigated when the plate is deformed in a microwave field with a frequency in the range from (1...10) GHz. As shown by calculations (see Equations (18), (18a)), the shift of the NFMR frequency as a result of the stress effect can reach 20% before the destruction of the composite. Therefore, this effect can be used for contactless diagnostics of deformations in distant objects (including critical infrastructures) reinforced by cast magnetic microwires with the stress effect of NFMR. To this end, these objects are periodically scanned with a floating-frequency radar to determine the deviation of the initial NFMR frequency due to potentially dangerous deformations of the monitored object.

It is worth mentioning also another principle of detecting mechanical strain which is examined in Ref. [20]. This principle is based on the giant magnetoimpedance (GMI) effect (see Figure 9),so that it is different from that presented in Figure 8a.The GMI effect demands external magnetization of the sample which is not required in the NFMR method (see Refs. [2-8]).

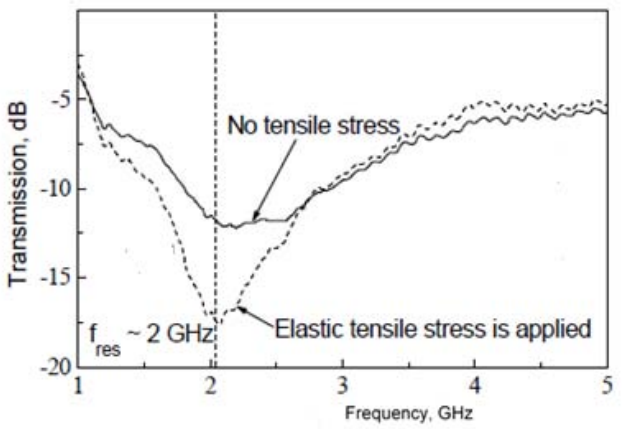

Figure 9: Stress dependence of the transmission coefficient for a single-layer composite sample measured in the free-space near field (see Ref. [20])

According to the above, the proposed method (based on the NFMReffect) is more technologically advanced than the method based on the GMI effect.

V. Conclusion

The microwave electromagnetic response has been analyzed for a composites consisting of dipoles and diffraction grating of amorphous magnetic glass-coated microwires in a dielectric. Thys materials can be employed for radio absorbing screening. The spontaneous NFMR phenomena observed in glass-coated microwires has opened the possibility of developing novel materials with broad-band of radio absorbing materials.

The described studies provide the following basic conclusions.

(A) We have derived simple analytical expressions for residual and mechanical stresses in the metallic core of the microwire, which clearly show their dependence on the ratio of the external radius of the microwire to the radius of the metal core and on the ratio of Young's moduli of the glass and the metal. Our modeling based on the theory of thermoelastic relaxation shows that the residual stresses increase from the axis of the microwire to the surface of the microwire metallic core, which is in accordance with the previously obtained experimental data (see [2]). Thus, in the case of glass-coated cast microwires prepared by the Taylor–Ulitovsky method, the residual stresses achieve maximum values on the surface of the metal core (see [2–8]).

(B) Cast GCAMNWs exhibit NFMR, whose frequency depends on the composition, geometrical parameters, and deformation of the microwire. The NFMR phenomenon observed in glass-coated magnetic microwires opens up the possibility of developing new radio-absorbing materials with a wide range of properties. An important feature of cast microwires with an amorphous magnetic core is the dependence of the NFMR frequency on the deformation (stress effect). The calculations have shown (see (18), (18a)) that the shift of the NFMR frequency caused by the stress effect bc an achieve 20% before the degradation of the composite.

(C) This effect can be used for contactless diagnostics of deformations in distant objects (including critical infrastructures) reinforced by cast magnetic microwires with the stress effect of NFMR. To this end, these objects are periodically scanned with a floating-frequency radar to determine the deviation of the initial NFMR frequency due to potentially dangerous deformations of the monitored object.

(D) The overall technology of magnetic wire composites is cost-effective and is suitable for large-scale applications.

Here we have discussed the electromagnetic properties of composites with magnetic wires showing NFMR phenomena. A striking property of these materials is that the spectra of the effective electromagnetic parameters (permittivity and permeability) can be actively tuned.

Technology of glass coated amorphous and nanocrystalline microwires allows the fabrication of continuous wires

Appendix A.Scheme for measuring the radio-absorbing properties

The material parameters in microwaves frequencies usually are found from the measurement of the reflection and/or transmission coefficients from which the complex permittivity (permeability) are calculated.

The measurement methods can be divided in two categories:

1) Transmission line methods (coaxial lines probes, rectangular waveguides, cavity resonators ((see Ref. [15]). Thus methods (in the first category) require cutting a piece of a sample to be placed inside the transmission line or cavity making a close contact with the probe. The transmission line methods work best for homogeneous materials that can be precisely machined to fit inside the sample holder.
2) Antenna techniques in free space (see below).

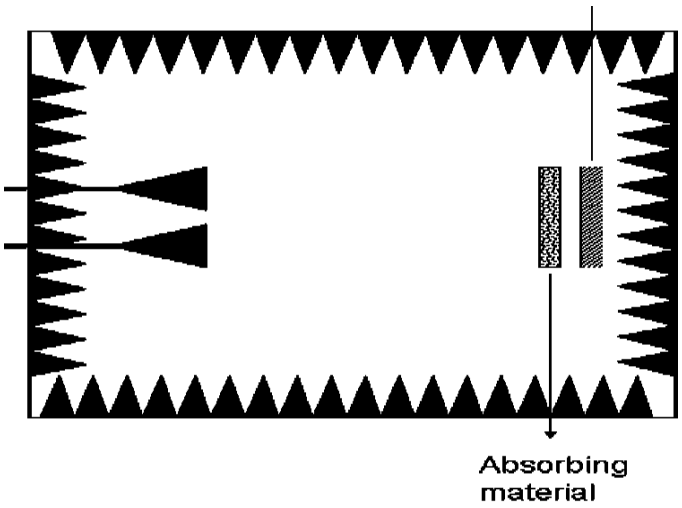

Figure A: A variant of the experimental scheme for microwave measurements

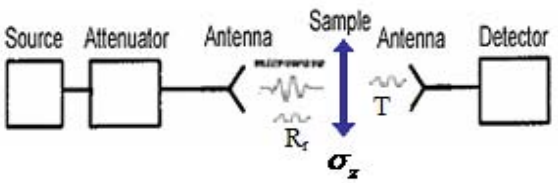

Figure A1: Scheme for measuring the radio-absorbing properties of samples with EFMR (according [2, 6, 19]) under the influence of external mechanical stresses

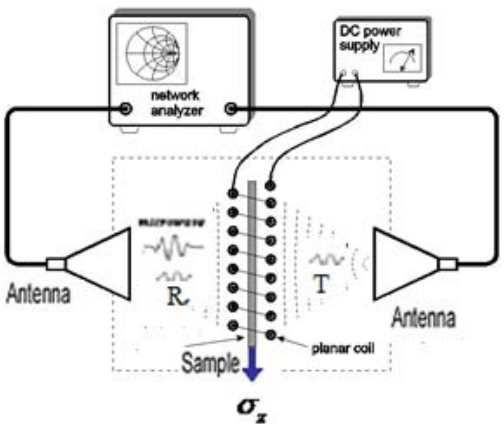

Figure A2: Scheme for measuring the radio-absorbing properties of sampleswith GMI (according [20]) under the influence of external mechanical stresses

Let's examine the simple theory of measurement of radio absorbing composition materials

It is well known, that the simple model of contact of vacuum with the absorbing material gives the following equations [2, 5, 19]

$$1+ R_r = T, \qquad \text{(A. 1)}$$

$$(\alpha+i\beta)(1- R_r)= T;$$

that gives

$$R_r = \frac{1-\alpha-i\beta}{1+\alpha+i\beta}, \qquad \text{(A. 2)}$$

and at $\beta = 0$, $\alpha = 1$, we find

$$R_r = 0. \qquad \text{(A. 3)}$$

From these it is possible to obtain a simple criterion for matching of vacuum with a radio absorbing material:

$$\mu_m \sim \Sigma_m / \Omega, \qquad \text{(A. 4)}$$

(where μ_m is effective magnetic permeability of composite). This condition cannot be satisfied for composites containing amorphous magnetic wires. This forces us to use other physical principles for creation of radio absorbing materials presented above).

We note that similar results were obtained in Refs. [2, 7, 8, 19].

References Références Referencias

1. G. F. Taylor, *Phys. Rev.* 1924, *23*, 655, DOI10.1103/PhysRev.23.655.
2. S. A. Baranov. An engineering review about microwire. Lambert (Academic publishing) 2017 pp. 1- 42
3. A. N. Antonenko, S. A. Baranov, V. S. Larinand A.V. Torcunov, Rapidly quenched & metastable materials, supplements to Materials Science and Engineering A (1997) 248.
4. S. A. Baranov, V. S. Larin, A. V. Torcunov, *Crystals* 2017, 7, 136, DOI 10.3390/cryst7060136.
5. S.A. Baranov, J. Commun. Techn.Electron.48 2 (2003) 226.
6. S. A. Baranov, *Tech. Phys. Lett.* 1998, *24*,549, DOI 10.1134/1.1262189.
7. S. A. Baranov, M. Yamaguchi, K. L. Garcia, M. Vazquez, *Surf. Engin. Appl. Electrochem.* 2008, *44*,245, DOI 10.3103/S106837550806001X.
8. S. A. Baranov, *Moldavian J. Phys. Sci.*, 2015, *14*, 201, http://nano.asm.md/uploads/moldphys/2015/moldphys2015v14n34.pdf.
9. P. Marín, D. Cortina, A. Hernando, *J. Magn. Magn. Mater.* 2005, *290–291*, 1597, DOI 10.1016/j.jmmm.2004.11.255.
10. H.-X. Peng; F. Qin; M.-H. Phan, in *Ferromagnetic microwires composites: from sensors to microwave applications*, Springer, Switzerland 2016, Ch. 12-14.
11. F. Qin, H.-X. Peng, *Progr. Mater. Sci.* 2013, *58*, 181, DOI 10.1016/j.pmatsci.2012.06.001.
12. L. Kraus, G. Infante, Z. Frait, M. Vázquez, *Phys. Rev. B* 2011, *83*, 174438, DOI 10.1103/PhysRevB.83.174438.
13. L. Kraus, *Czech. J. Phys.*1982, *32*, 1264, DOI 10.1007/BF01597425.
14. O. Reynet, A.-L. Adenot, S. Deprot, O. Acher, M. Latrach, *Phys. Rev. B* 2002, *66*,094412, DOI 10.1103/PhysRevB.66.094412.
15. S. N. Starostenko, K. N. Rozanov, A.V.Osipov, *J. Magn. Magn. Mater.* 2006, *298*,56, DOI 10.1016/j.jmmm.2005.03.004.
16. F. Yıldız, B. Z .Rameev, S. I. Tarapov, L. R. Tagirov, B. Aktaş, *J. Magn. Magn. Mater.* 2002, *247*, 222, DOI 10.1016/S0304-8853(02)00187-7.
17. D .Ménard, M. Britel, P. Ciureanu, A. Yelon, *J. Appl. Phys.*1998, *84*,2805, DOI 10.1063/1.368421.
18. D. Ménard, A. Yelon, *J.Appl.Phys.*2000, *88*,379, DOI 10.1063/1.373671.
19. E. Adar, A. M. Yosher, S. A. Baranov, J. Phys Res Appl. 2020; 3: 118-122. DOI: 10.29328/journal.ijpra.1001028.
20. D. Makhnovskiy, A. Zhukov, V. Zhukova, J. Gonzalez, *Adv. Sci. Technol.* 2008, *54*, 201, DOI 10.4028/www.scientific.net/AST.54.201.